Check for updates

LncRNA FGD5-AS1 promotes the malignant phenotypes of ovarian cancer cells via targeting miR-142-5p

Zhang Aichen[1] · Wang Kun[1] · Sun Xiaochun[1] · Tong Lingling[1] (ORCID)

Abstract

Long non-coding RNAs (lncRNAs) have been reported to participate in regulating gene expression and are related to tumor progression. FGD5 antisense RNA 1 (FGD5-AS1) facilitates the progression of various tumors. However, the expression and function of FGD5-AS1 in ovarian cancer (OC) and its mechanism of action are not yet clear. Real-time polymerase chain reaction (RT-PCR) was employed to explore the expression levels of FGD5-AS1 and miR-142-5p in OC. The relationship between the expression of FGD5-AS1 and clinicopathological indicators of OC patients was analyzed by χ^2 test. CCK-8 assay, BrdU assay, and Transwell assay were carried out to detect cell proliferation, migration, as well as invasion, respectively. Subcutaneous tumorigenesis experiment and lung metastasis model were used to examine the biological effects of FGD5-AS1 in OC in vivo. Dual luciferase reporter gene assay or RIP experiment was employed to explore the targeting relationship between FGD5-AS1 and miR-142-5p, as well as miR-142-5p and PD-L1 3′UTR. First, we found that FGD5-AS1 was markedly up-regulated in OC. Moreover, its high expression level was associated with positive local lymph node metastasis and higher T stage in OC patients. Gain-of-function and loss-of-function assays demonstrated that FGD5-AS1 facilitated the proliferation, migration, as well as invasion of OC cells. Mechanistically, it was revealed that FGD5-AS1 targeted miR-142-5p to repress its expression and function. Furthermore, miR-142-5p has a binding site for 3' UTR of PD-L1, and FGD5-AS1 could positively regulate PD-L1 expression via repressing miR-142-5p. The present study reports that FGD5-AS1/miR-142-5p/PD-L1 axis is involved in regulating OC progression.

Graphic abstract

Ovarian Cancer Cell
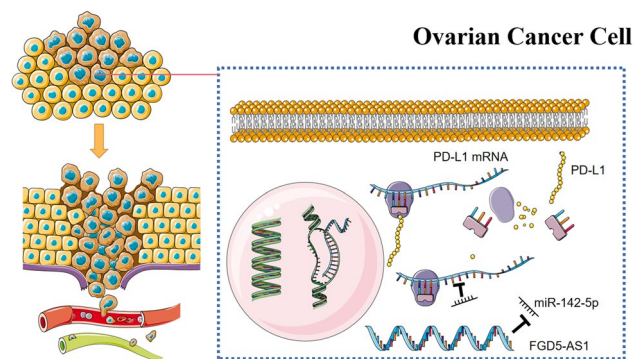
✉ Sun Xiaochun
xcsun@jlu.edu.cn

✉ Tong Lingling
tongll16@mails.jlu.edu.cn

[1] Department of Obstetrics and Gynecology, The Third Hospital of Jilin University, 126th Xiantai Street, Changchun 130021, Jilin, China

Introduction

Ovarian cancer (OC) is one of the most common gynecological malignant tumors of the female reproductive system [1, 2]. Many patients with OC are not diagnosed until the

advanced stage, and OC has a high potential for relapse and metastasis, so the prognosis is extremely poor [3, 4]. Hence, exploring valuable biomarkers and therapeutic targets is of great significance to the patients with OC.

Long non-coding RNA (lncRNA) is characterized as a transcript of more than 200 nucleotides and once considered as a by-product of genome transcription [5, 6]. Increasing evidence demonstrates that lncRNA can modulate the expression of target genes through various mechanisms [7]. In cancer biology, the dysregulation of lncRNA is involved in facilitating or repressing tumorigenesis and cancer progression [8–12]. For example, lncRNA MNX1-AS1 facilitates the proliferation, migration, invasion, as well as epithelial-mesenchymal transition of bladder cancer cells by up-regulating RAB1A expression [10]; LncRNA LUADT1 boosts the migration and invasion of small cell lung cancer by up-regulating the expression of TWIST1 [11]. Up to now, the role of lncRNA FGD5 antisense RNA 1 (FGD5-AS1) in OC is unclear.

MicroRNAs (miRNAs) are a kind of small endogenous single-stranded non-coding RNAs composed of 19–25 nucleotides [13, 14]. MiRNA participates in the regulation of target gene expression through binding with 3′-untranslated region (3′-UTR) [15–17]. MiR-142-5p is a cancer-related miRNA. It targets Sorbin and SH3 domain-containing protein 1, and facilitates the metastasis of breast cancer cells [18]. What's more, miR-142-5p impedes the malignant progression of lung adenocarcinoma by negatively regulating the expression of CDK5 [19]. Nevertheless, the expression and mechanism of action of miR-142-5p in OC are rarely studied. It is worth noting that bioinformatics analysis suggests the existence of potential binding site between FGD5-AS1 and miR-142-5p, indicating that FGD5-AS1 can probably function as the molecular sponge of miR-142-5p.

Known as CD274, programmed cell death ligand-1 (PD-L1) is a type I transmembrane glycoprotein consisting of 290 amino acid residues, and is the main ligand of programmed death 1 (PD-1) [20]. PD-L1 is an immunomodulatory protein and induces tumor cells to escape immunity by suppressing the immune response [21]. Many studies indicate that PD-L1 expression markedly rises in a variety of malignant tumor tissues and cell lines, which induces the apoptosis of immune cells, thereby promoting the occurrence and progression of tumors [22–24]. PD-L1 is highly expressed in the OC cell membrane and cytoplasm, and PD-L1 inhibitors have potential to treat OC [25]. However, the upstream mechanism of dysregulation of PD-L1 in OC still needs further study.

The expression, clinical significance, as well as function of FGD5-AS1 were explored in OC in this study. This study confirmed for the first time that FGD5-AS1 facilitated the proliferation and metastasis of OC cells with in vivo and in vitro experiments. Mechanistically, this study found that FGD5-AS1 facilitated OC progression by modulating miR-142-5p/PD-L1 expression. This study deepens the understanding of the mechanism of OC progression, which might offer new targets for the treatment of ESCC.

Material and methods

Patients and tissue samples

This study got approval of the Research Ethics Committee of The Third Hospital of Jilin University. OC patients underwent tumor resection at The Third Hospital of Jilin University from June 2017 to June 2019, and all of them signed an informed consent form. 52 cases of OC tissue specimens and adjacent normal tissues (3 cm away from the tumor margin) were obtained and immediately stored in liquid nitrogen. None of the patients received radiotherapy, chemotherapy, and molecular targeted drugs prior to tissue collection.

Cell culture

Human OC cell lines (OVCAR3, SKOV3, HO8910, A2780, and COV644 cells) and normal ovarian epithelial cell line (IOSE cells) were available from the Chinese Academy of Sciences (Shanghai, China). Moreover, these cells were inoculated in Roswell Park Memorial Institute (RPMI) -1640 (Gibco, Carlsbad, CA, USA), in which 10% FBS (Invitrogen, Carlsbad, CA, USA) and 100 U/mL penicillin and 0.1 mg/mL streptomycin (Sigma- Aldrich, St. Louis, MO, USA) were added, and cells were then cultured at 37 °C in 5% CO_2. When cells confluence grew to about 80%, the cells were trypsinized with 0.25% trypsin (Thermo Fisher HyClone, Utah, USA) for subculture.

Cell transfection

The FGD5-AS1 overexpression plasmid, FGD5-AS1 small interfering RNA (si-FGD5-AS1), and their negative controls were designed and synthesized by GeneChem (Shanghai, China). miR-142-5p mimics or miR-142-5p inhibitors and their negative controls were available from Ribobio (Guangzhou, P.R. China). 2×10^4 cells per well were inoculated into a 6-well plate, and after 24 h of culture, the medium was then discarded. According to the manufacturer's instructions, OVCAR3 cells and HO8910 cells were then transfected with Lipofectamin®3000 (Invitrogen, Carlsbad, CA, USA).

RNA isolation and quantitative real-time polymerase chain reaction (RT-PCR)

Total RNA was extracted employing TRIzol reagent (Invitrogen, Carlsbad, CA), and subsequently reversely

transcribed into complementary DNA (cDNA) employing reverse transcription kit (Applied Biosystems, Foster City, CA, USA). SYBR® Premix-Ex-Taq kit (Takara, Dalian, China) and RT-PCR detection system were utilized to perform RT-PCR. The relative expressions of FGD5-AS1, miR-142-5p, and PD-L1 were calculated employing the $2^{-\Delta\Delta CT}$ method. The primer sequences were available from Genecopoeia (Guangzhou, China) (Table 1).

Evaluation of cell proliferation

Each group of cells was trypsinized with 0.25% trypsin to prepare single cell suspension. Moreover, after counting the number of the cells, the cells were inoculated in a 96-well plate (approximately 2×10^3 cells per well) and then placed in an incubator for culture. After the cells were cultured for 1, 2, 3, 4, and 5 days, cell counting kit-8 assay (CCK-8) reagent (Beyotime Biotechnology, Shanghai, China) were added in each well, and the cells were incubated for 2 h. Finally, TECAN infinite M200 Multimode microplate reader (Tecan, Mechelen, Belgium) was employed to detect the absorbance of each well at 450 nm wavelength.

In BrdU assay, briefly, the cells were inoculated into a 96-well plate with 1000 cells per well for culture for 24 h, followed by adding BrdU solution (Beyotime, Shanghai, China). After 24 h of culture, 100 μL of fixative solution was added. 30 min later, the cells were rinsed three times and then blocked with 10% bull serum albumin (BSA) for 30 min. After the cells were rinsed, anti-mouse BrdU monoclonal antibody (Abcam, ab8152, 1: 300) was added to incubate the cells for 1 h at room temperature. Next the cells were stained with DAPI to label the nuclei, and then the cells were observed under a fluorescence microscope and counted.

Table 1 The sequences used for qRT-PCR

Name	Primer sequences
FGD5-AS1	Forward: 5′-GAAGGGCCGAAGAG CTCAAT-3′
	Reverse: 5′-GGCTCGCAAAGTGTCTGTTG-3′
miR-142-5p	Forward: 5′-CATAAAGTAGAAAGCACTAC-3′
	Reverse: 5′-GAACATGTCTGCGTATCTC-3′
U6	Forward: 5′-AGATTAGCATGGCCCCTGC-3′
	Reverse: 5′-GCAGGGGCCATGCTAATCT-3′
PD-L1	Forward: 5′- CAAATGTTGTTTGGGTCATGC -3′
	Reverse:5′-GTAAAACGACGGCCAGTCATTCCT TCCTCTTGTCACGC -3′
GAPDH	Forward: 5′- GGCATGGACTGTGGTCATGAG -3′
	Reverse: 5′- TGCACCACCAACTGTTAGC -3′

Evaluation of cell migration and invasion

Transwell experiment was utilized to evaluate cell migration and invasion. The cells were trypsinized with trypsin and collected. The cells were then re-suspended in serum-free RPMI-1460 medium. The cells were then added to the upper chamber of Transwell system (BD Biosciences, San Jose, CA, USA) (2×10^5 cells/well), and the lower chamber was added with 600 μL of culture solution containing 20% FBS. Subsequently, the cells were placed in an incubator at 37 ℃ in 5% CO_2 for 24 h. After the cells remaining on the upper surface of membrane were removed, the cells on the bottom of the membrane were fixed with 4% paraformaldehyde, and then stained with 0.1% crystal violet solution. After washed and dried, the cells were photographed and counted. In cell invasion experiment, except that the upper chamber of Transwell needed to be coated with Matrigel in advance before adding cells, the rest steps were as the same as those in the migration experiment.

Western blot

Cells in each group were added with RIPA lysis buffer (Beyotime Biotcchnology, Shanghai, China) to extract the total protein of cells in each group. After centrifugation (12000 r/min, 15 min), the supernatant was collected as the protein sample. BCA Protein Assay Kit (Pierce, Rockford, IL, USA) was utilized to assess protein concentration. The total protein was subsequently separated by SDS-PAGE, and the protein samples were then transferred to polyvinylidene fluoride (PVDF) membrane. After that, the membrane was blocked with 5% skim milk for 1 h. Moreover, primary antibody anti-PD-L1 antibody (Abcam, ab205921, 1: 1000) was added to incubate the membrane at 4 ℃ overnight. The next day, Tris-buffered saline-Tween (TBST) was utilized to rinse the membrane. After that, the secondary antibody (horseradish peroxidase-labeled goat anti-rabbit IgG, 1: 2000) was added to incubate the membrane at 37 ℃ for 1 h. After the membrane was washed by TBST again, the protein bands were developed by electrochemiluminescence (ECL) kit (Millipore, Bedford, MA, USA).

Dual-luciferase reporter assay

Online bioinformatics databases (StarBase, TargetScan) were employed to predict the target fragments between FGD5-AS and miR-142-5p, as well as miR-142-5p and PD-L1 3′-untranslated region (3′-UTR). The wild type (WT) and mutant type (MUT) FGD5-AS1 fragments and WT and MUT sequences from the 3′UTR of PD-L1 were integrated into the luciferase reporter vector pmirGLO (Promega, Madison, WI, USA). Moreover, luciferase plasmids, miR-142-5p mimics or negative control were co-transfected

into OVCAR3 and HO8910 cells. Subsequently, 48 h after the transfection, the luciferase activity of the cells was subsequently measured employing the Dual-Luciferase Reporter Assay System (Promega, Madison, WI, USA) according to the manufacturer's instructions.

RNA immunoprecipitation (RIP) assay

EZMagna RIP kit, human anti-Argonaute 2 (anti-Ago2 antibody), the anti-IgG (used as control) were purchased from Millipore (Billerica, MA, USA). RIP analysis was performed, which was based on the manufacturer's protocol, and NanoDrop spectrophotometer was employed to examine RNA concentration. Finally, RT-PCR was conducted to analyze the enrichment of FGD5-AS1 and miR-142-5p in the immunoprecipitate.

In vivo experiments

Female BALB/c nude mice (6-week-old, 20 g, Charles River Laboratories, Guangzhou, China) were housed in a pathogen-free facility with a temperature of 24 ± 1 °C, a humidity of 50%, 12-h light–dark cycle, and ad libitum access to water and food. After one week of acclimation, animals were randomly divided into two groups: control group and FGD5-AS1 knockdown group. The procedures in animal experiments got approval from the Animal Model Research Center, China-Japan Union Hospital of Jilin University. Moreover, HO8910 cells in si-con group and si-FGD5-AS1 group in the logarithmic growth phase were harvested. Subsequently, after the cells were rinsed with PBS and resuspended, the cell concentration was modulated to 2×10^8/ml. Cell suspension (0.1 mL per mouse) was injected subcutaneously in the back of nude mice to construct a model of subcutaneous xenograft tumor in nude mice (10 mice per group). The general condition and tumor volume of nude mice were observed, and the longest diameter (a) and the shortest diameter (b) of the tumor were measured with a vernier caliper. The tumor volume was calculated: $V = ab^2 \times 0.5$, and tumor growth curve was made. Nude mice were euthanized after 5 weeks and the tumors were weighed. To establish a lung metastasis model, 2×10^7 HO8910 cells (si-con or si-FGD5-AS1) were injected into each mouse via caudal vein (10 mice per group). After 2 weeks, the mice were euthanized, and the lungs were taken for hematoxylin–eosin (HE) staining.

HE staining

The paraffin was removed from the slices with xylene, and the tissues were hydrated through high-concentration to low-concentration ethanol (95%, 90%, 80%, and 70%). After adding distilled water, the sections were subsequently put into hematoxylin staining solution for stain for 3 min.

Furthermore, the colors were separated. Then, the sections were rinsed with running water for 1 h and put into distilled water for 1 min. After dehydrating in 70% and 90% ethanol respectively for 10 min, the sections were stained with eosin staining solution for 2 min, and then dehydrated with anhydrous ethanol. Subsequently, the sections were made transparent with xylene, and finally the sections were sealed. Pathological characteristics were observed under an inverted microscope.

Statistical analysis

The data were all processed by SPSS 19.0 software (SPSS Inc., Chicago, IL, USA). The data were expressed by "mean $\pm$ standard deviation" ($x \pm s$). The differences in the data among multiple groups were compared employing one-way ANOVA and LSD test. The difference between the data of two groups was compared employing t test. $P < 0.05$ was considered to be statistically significant.

Results

The expression characteristics and clinical significance of FGD5-AS1 in OC

First of all, RT-PCR was employed to detect FGD5-AS1 expression in 52 pairs of OC samples. The results showed that compared with that of non-tumor tissues, FGD5-AS1 expression in OC tissue was markedly up-regulated (Fig. 1a). Furthermore, the expression of FGD5-AS1 in normal ovarian epithelial cells (IOSE cells) and OC cell lines (OVCAR3, SKOV3, HO8910, A2780, and COV644 cells) was also examined. RT-PCR results showed that compared with in IOSE cells, the expression of FGD5-AS1 in above five OC cell lines was also observably up-regulated (Fig. 1b). Moreover, and the median of FGD5-AS1 expression level in cancer tissues of 52 patients was used as a standard to differentiate high expression and low expression groups. χ^2 test indicated that the expression of FGD5-AS1 was positively correlated with T stage and local lymph node metastasis (Table 2). These research data hinted that FGD5-AS1 exerted an impact on promoting OC progression.

FGD5-AS1 facilitated OC cell proliferation, migration, and invasion in vitro

The data mentioned above implied that among the five types of cells (OVCAR3, SKOV3, HO8910, A2780, and COV644 cells), FGD5-AS1 expression was the lowest in OVCAR3 cells, while the highest in HO8910 cells (Fig. 1b). Therefore, FGD5-AS1 overexpression plasmid was transfected into OVCAR3 cells, and the FGD5-AS1 expression in HO8910
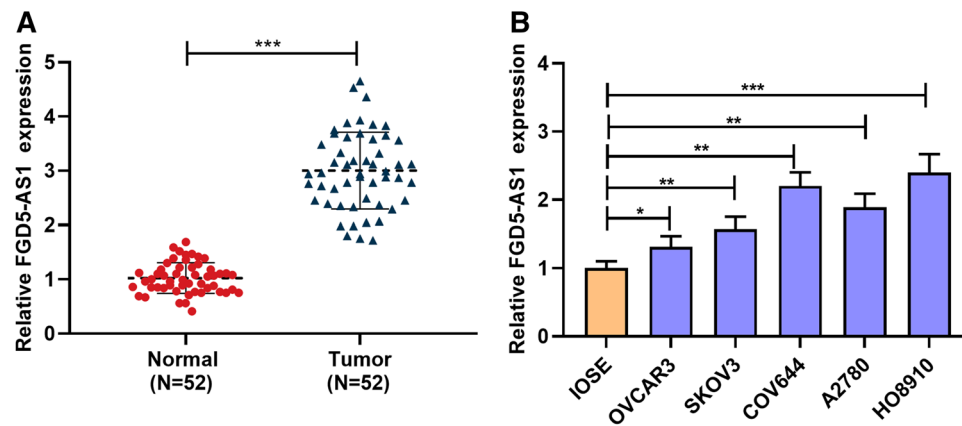
Fig. 1 Expression of FGD5-AS1 in OC. **a** RT-PCR was employed to verify the expression level of FGD5-AS1 in human OC tissues and normal tissues adjacent to cancer (Total = 52). **b** RT-PCR was utilized to access the expression of FGD5-AS1 in normal ovarian epithelial cells (IOSE cells) and five OC cells (OVCAR3, SKOV3, HO8910, A2780, and COV644 cells). *symbolizes $P < 0.05$, **symbolizes $P < 0.01$, and ***symbolizes $P < 0.001$

Table 2 The relationships between FGD5-AS1 expression and clinicopathological factors of OC

| Clinicopathologic factors	Patients number (n = 52)	FGD5-AS1 expression		χ^2	p
		Lower (n = 26)	Higher (n = 26)		
Age				0.0799	0.7775
≤ 50	31	16	15		
> 50	21	10	11		
Tumor size(cm)				1.9490	0.1627
≤ 3	29	12	17		
> 3	23	14	9		
Tumor histology				0.8976	0.6384
Serous	15	9	6		
Mucinous	16	7	9		
Endometroid	21	10	11		
Lymph node metastasis				3.9140	0.0479*
No	21	14	7		
Yes	31	12	19		
T stage				5.0424	0.0247*
I–II	30	19	11		
III	22	7	15		

*p < 0.05

cells was knocked down with siRNA, and RT-PCR confirmed that the over-expression and knock-down model was successfully constructed (Fig. 2a). The results of CCK-8 and BrdU experiments illustrated that compared with the control group, FGD5-AS1 overexpression facilitated the proliferation of OVCAR3 cells (Fig. 2b, c). Subsequently, Transwell experiment was conducted, and it was found that FGD5-AS1 overexpression promoted the migration and invasion of OVCAR3 cells (Fig. 2d, e). In the contrary, knocking down FGD5-AS1 markedly repressed the proliferation, migration, as well as invasion of HO8910 cells (Fig. 2b–e). Besides, in order to investigate the role of FGD5-AS1 on normal cells

(IOSE cells), FGD5-AS1 overexpression plasmid and si-FGD5-AS1 were transfected into IOSE cells, respectively (Supplementary Fig. 1a). The results of CCK-8 showed that neither up-regulation of FGD5-AS1 nor down-regulation of FGD5-AS1 significantly affected the proliferation of IOSE cells compared with the control group (Supplementary Fig. 1b).

FGD5-AS1 directly targeted miR-142-5p

LncRNA often participates in regulating malignant progression of tumors by adsorbing miRNAs. To explore
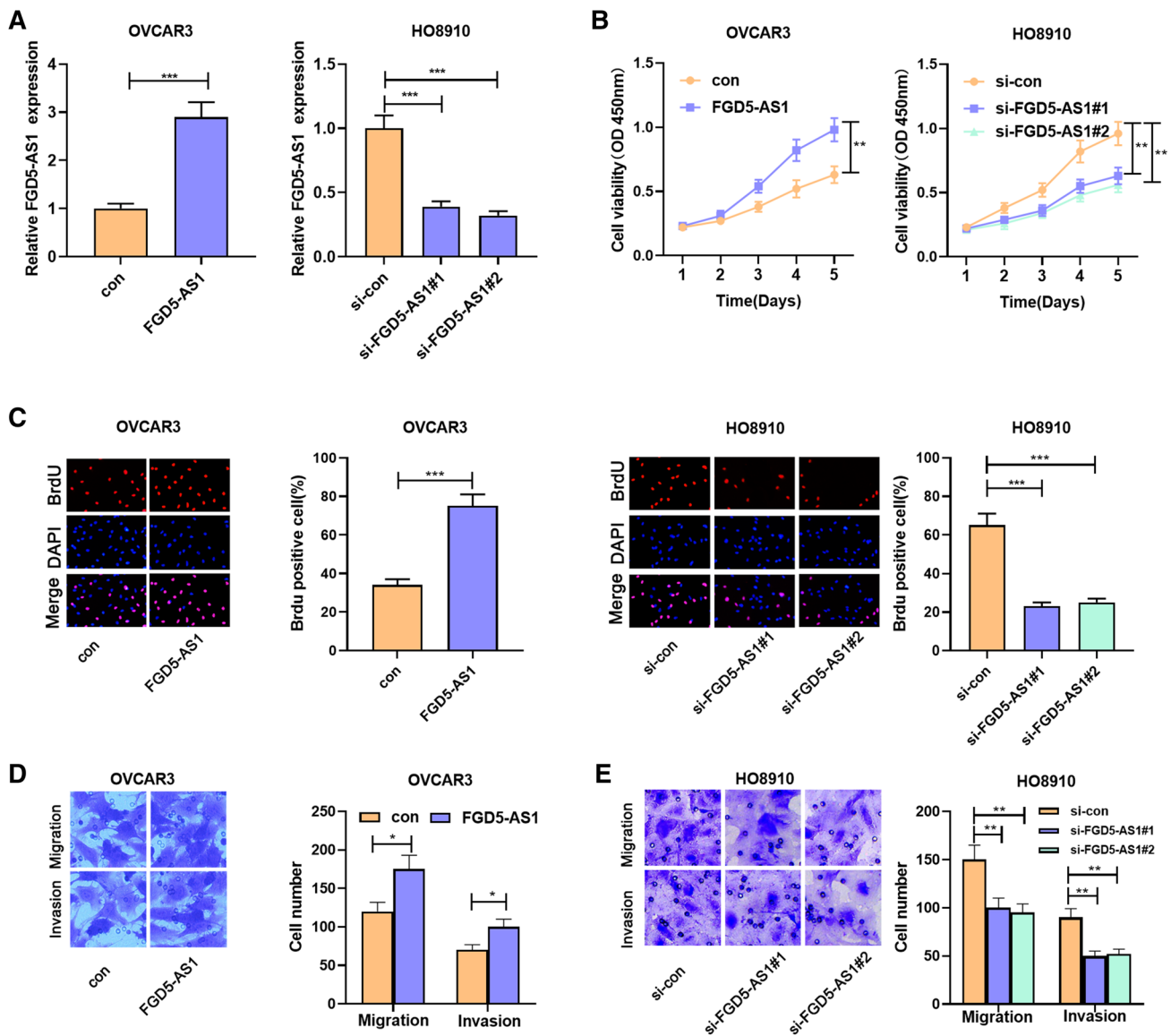
Fig. 2 FGD5-AS1 facilitated OC cell proliferation, migration, and invasion in vitro. **a** FGD5-AS1 overexpressed plasmid and si-FGD5-AS1 were transfected into OVCAR3 cells and HO8910 cells respectively, and the transfection efficiency was verified by RT-PCR. **b** and **c** CCK-8 experiment and BrdU experiment were employed to examine the proliferation of OC cells. **d** and **e** Transwell assay was employed to examine OC cell migration and invasion. *symbolizes $P < 0.05$, **symbolizes $P < 0.01$, and ***symbolizes $P < 0.001$

the downstream mechanism of FGD5-AS1, StarBase online database was utilized, and a potential binding site between FGD5-AS1 and miR-142-5p was found (Fig. 3a). Interestingly, there was a negative relationship between FGD5-AS1 expression and miR-142-5p expression in OC samples (Fig. 3b). Then dual luciferase reporter gene experiment was performed, and the result illustrated that compared with in the control group, miR-142-5p mimics could markedly inhibit the luciferase activity of the wild type FGD5-AS1 reporter, but no remarkable change was found in the luciferase activity of the mutant type

FGD5-AS1 reporter (Fig. 3c). Furthermore, RIP experiment confirmed that compared with the IgG immunoprecipitate, FGD5-AS1 and miR-142-5p were enriched in Ago2 immunoprecipitate (Fig. 3d). Additionally, RT-PCR results suggested that FGD5-AS1 overexpression in OVCAR3 cells markedly repressed miR-142-5p expression, while knockdown of FGD5-AS1 in HO8910 cells induced an increase in miR-142-5p expression level (Fig. 3e). Collectively, it was confirmed that miR-142-5p in OC cells was a downstream target of FGD5-AS1.
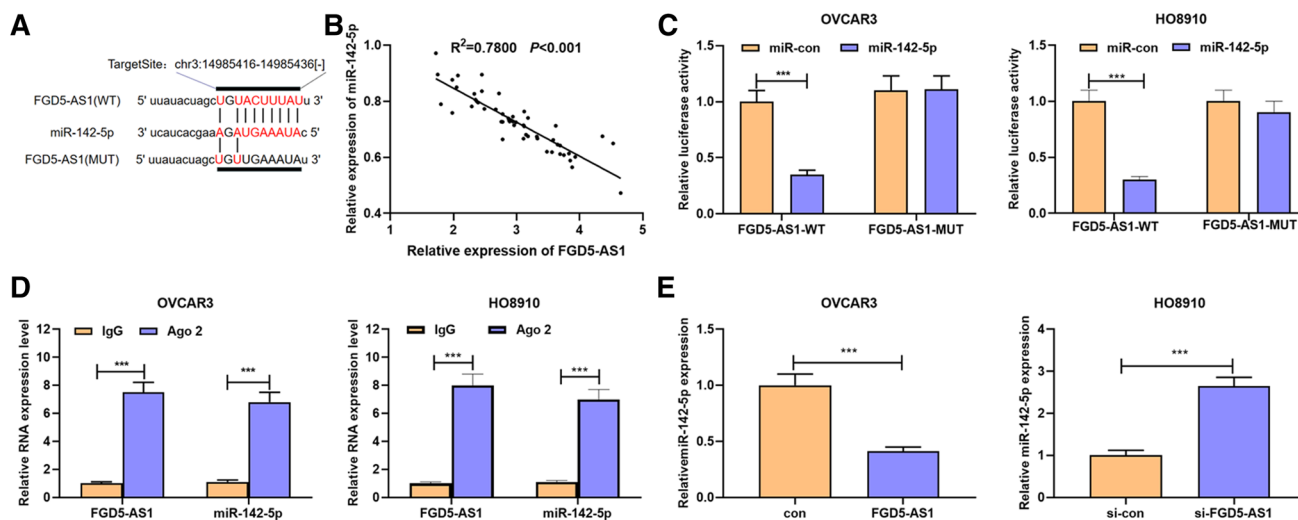
Fig. 3 miR-142-5p was the target of FGD5-AS1. **a** Bioinformatics predicted the binding site between FGD5-AS1 and miR-142-5p. **b** RT-PCR indicated that the expressions of FGD5-AS1 and miR-142-5p were negatively correlated in OC samples. **c** Dual luciferase report analysis suggested that miR-142-5p could impede the luciferase activity of wild type FGD5-AS1 reporter, but had no significant impact on the luciferase activity of mutant type FGD5-AS1 reporter. **d** RIP experiments verified the interaction between FGD5-AS1 and miR-142-5p. **e** After up-regulating FGD5-AS1 in OVCAR3 cells and knocking down FGD5-AS1 in HO8910 cells, RT-PCR was employed to investigate miR-142-5p expression. ***symbolizes $P < 0.001$

miR-142-5p repressed the malignant biological behaviors of OC cells

Next, the expression of miR-142-5p in OC tissues and cell lines was determined by RT-PCR. The results demonstrated that compared with adjacent normal tissues, the expression of miR-142-5p was markedly down-regulated in OC tissues and cell lines (Fig. 4a, b). To explore the biological role of miR-142-5p in OC, miR-142-5p overexpression model and low expression model were successfully constructed (Fig. 4c). The regulatory function of miR-142-5p in OC cell proliferation, migration, and invasion were then examined by CCK-8 experiment, BrdU experiment, as well as Transwell assay, respectively. It was found that up-regulation of miR-142-5p repressed cell proliferation, migration, as well as invasion (Fig. 4d–f), whereas the opposite effect was found after the inhibition of miR-142-5p expression (Fig. 4d–f). These results illustrated that miR-142-5p played a tumor-suppressive role in OC.

FGD5-AS1 participated in the regulation of OC cell progression by adsorbing miR-142-5p

To verify the role of FGD5-AS1/miR-142-5p axis in OC, miR-142-5p mimics were transfected into OVCAR3 cells with FGD5-AS1 overexpression, and miR-142-5p inhibitors were transfected into HO8910 with FGD5-AS1 knockdown (Fig. 5a). The proliferation, migration and invasion of OC cells were then assessed by CCK-8 experiment, BrdU experiment, as well as Transwell experiment. It was found that up-regulation of miR-142-5p partially weakened the promoting effects of FGD5-AS1 overexpression on OVCAR3 cell proliferation and metastasis, whereas the inhibitory effects of knocking down FGD5-AS1 on the malignant biological behaviors of HO8910 cells were partially reversed by miR-142-5p inhibitors (Fig. 5b–e). These results illustrated that FGD5-AS1 took part in the regulation of OC cell proliferation and metastasis by adsorbing miR-142-5p.

PD-L1 is the direct target of miR-142-5p in OC

Bioinformatics database (StarBase, TargetScan) were used to predict the target gene of miR-142-5p. Then, we used Venn diagram to identify the shared genes in the two datasets. A total of 702 potential target genes were screened (Fig. 6a). We performed KEGG pathway analysis to elucidate the potential biological functions of miR-142-5p integrated-signature. Interestingly, the KEGG pathways enriched for the miR-142-5p targets were mainly associated with cancer-specific pathways (Supplementary Fig. 2). Importantly, there was a potential binding site between miR-142-5p and the 3′UTR of PD-L1 (Fig. 6b). We performed a dual-luciferase reporter assay to determine the direct binding relationship between 142-5p and PD-L1 3′UTR in OC cells. The wild type and mutant type PD-L1 3′UTR reporters were constructed. Then, we co-transfected miR-142-5p mimics with the reporter vectors into OC cells. Compared with the mutant type group, after the transfection of miR-142-5p, a significant reduction in the luciferase activity of the wild type group was observed (Fig. 6c). In addition, the results of Western blot and RT-PCR showed that the
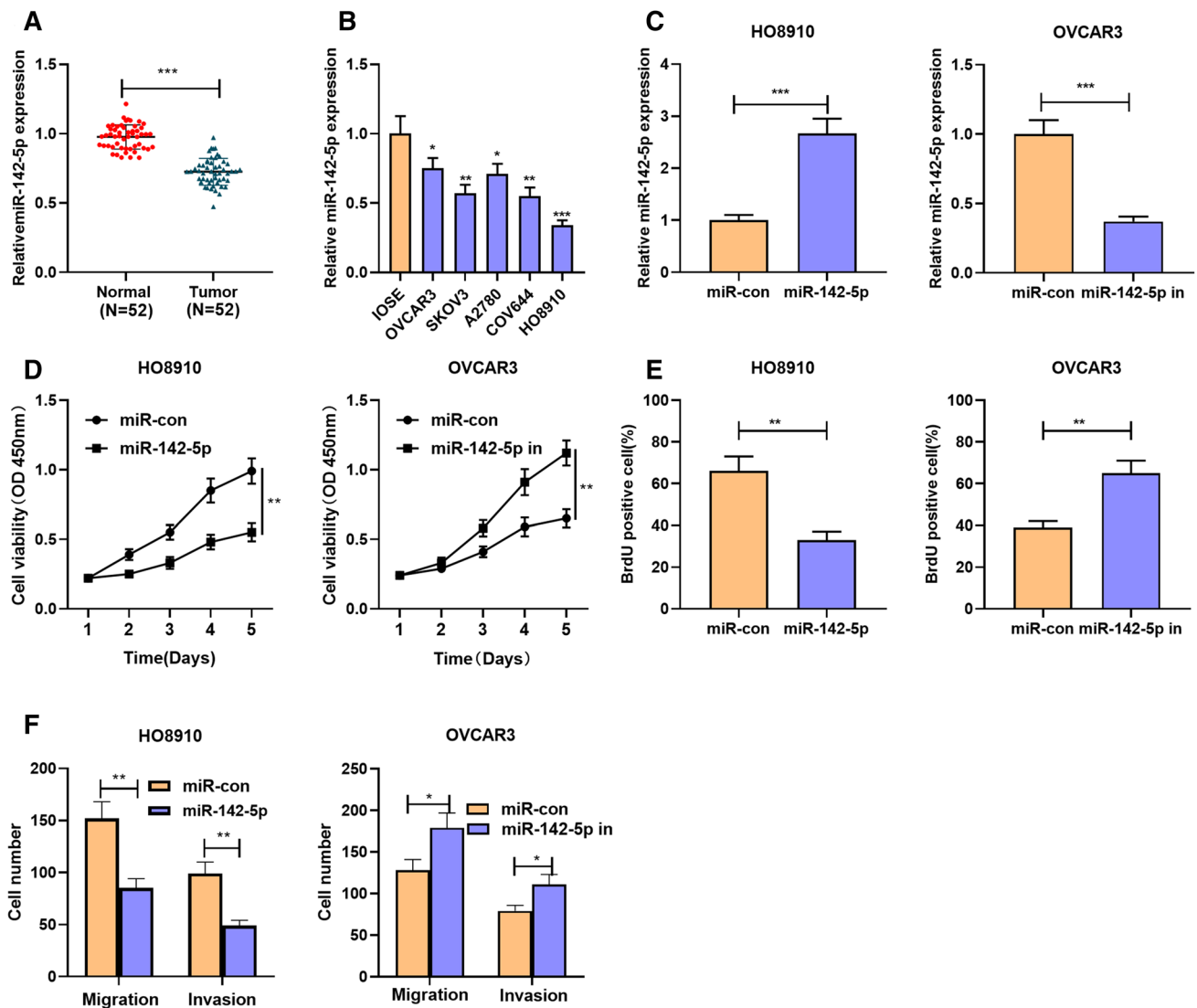
Fig. 4 miR-142-5p played a tumor suppressor role in OC proliferation and metastasis. **a** and **b** The expression of miR-142-5p in OC cancer tissues and cell lines was analyzed by RT-PCR. **c** miR-142-5p mimics and inhibitors were transfected into HO8910 cells and OVCAR3 cells, respectively, and RT-PCR was employed to detect the transfection efficiency. **d**–**f** miR-142-5p overexpression markedly repressed the proliferation, migration, and invasion of HO8910 cells, while down-regulation of miR-142-5p expression facilitated the above biological behaviors of OVCAR3 cells. *symbolizes $P<0.05$, **symbolizes $P<0.01$, and ***symbolizes $P<0.001$

expression level of PD-L1 could be negatively regulated by miR-142-5p and positively regulated by FGD5-AS1 (Fig. 6d, e). The expression of miR-142-5p was also verified to be negatively correlated with that of PD-L1, while a positive correlation between the expression of FGD5-AS1 and the expression of PD-L1 was observed (Fig. 6f, g). These data confirmed that PD-L1 was a direct target of miR-142-5p in OC cells.

Knocking down FGD5-AS1 repressed OC tumorigenesis in vivo

Furthermore, the function of FGD5-AS1 in vivo was explored. HO8910 cells transfected with si-con or si-FGD5-AS1 were inoculated on the back of each mouse to observe the tumor size and weight. Compared with the control group, the growth rate of tumor volume was markedly slowed down after knocking down FGD5-AS1 (Fig. 7a). Additionally, compared with the control group, the average weight of tumors in the si-FGD5-AS1 group was significantly reduced (Fig. 7b). RT-PCR results illustrated that miR-142-5p expression was increased markedly in the tumor tissues after knocking down FGD5-AS1 (Fig. 7c, d). RT-PCR and Western blot indicated that after FGD5-AS1 was knocked down, PD-L1 expression decreased at both mRNA and protein levels in tumor tissues (Fig. 7e, f). Moreover, a lung metastasis model was also established through tail
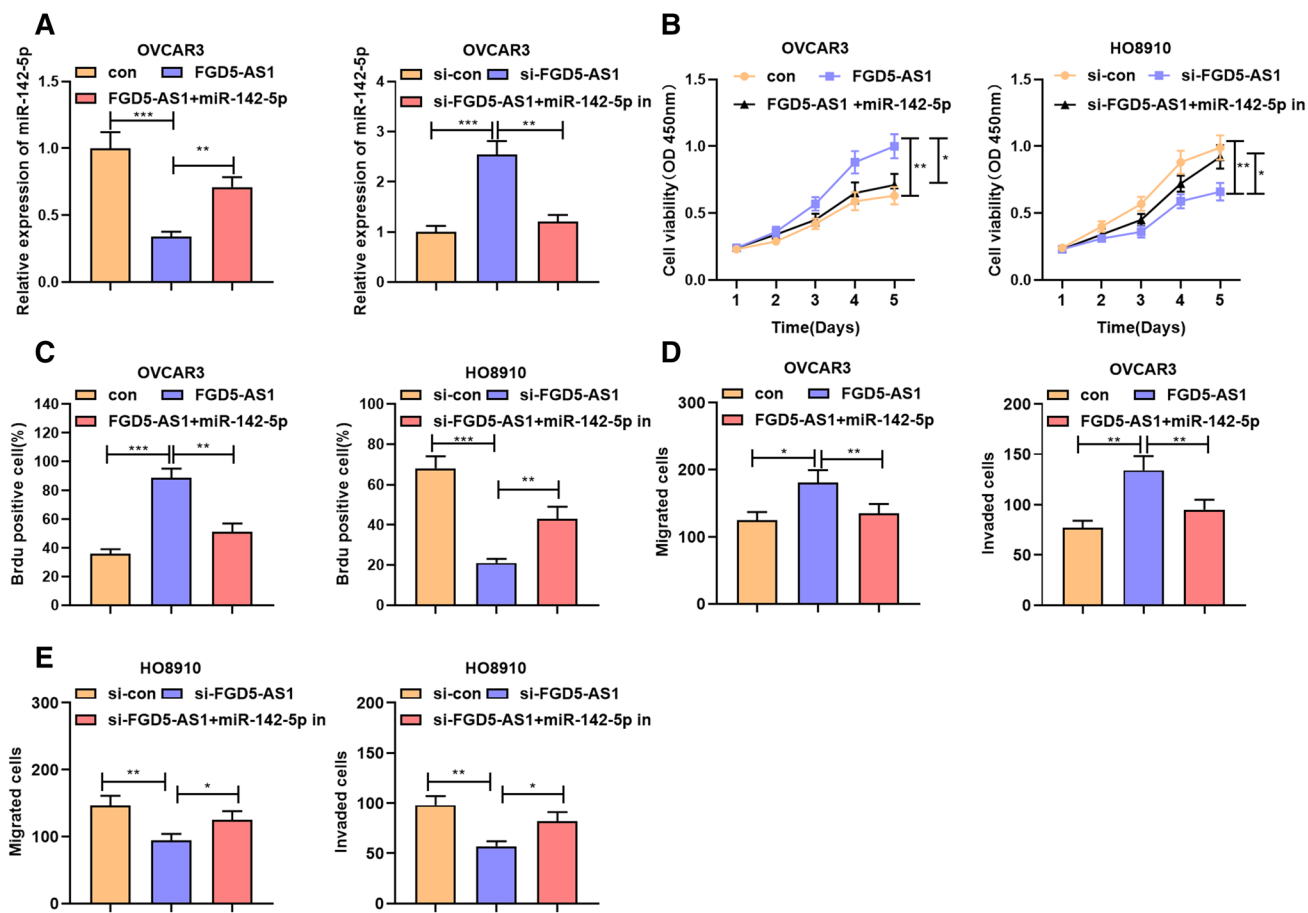
Fig. 5 FGD5-AS1/miR-142-5p was involved in the regulation of malignant progression of OC cells. **a** miR-142-5p mimics were transfected into OVCAR3 cells with FGD5-AS1overexpression. HO8910 cells with FGD5-AS1 knockdown were transfected with anti-miR-142-5p. RT-PCR was utilized to examine the expression of miR-142-5p in OC cells. **b–e** Upregulation of miR-142-5p weakened the promoting effects of FGD5-AS1 overexpression on OVCAR3 cell proliferation, migration, as well as invasion. Knocking down the expression of miR-142-5p reversed the inhibiting effects on proliferation, migration, and invasion of HO8910 cells caused by knocking down FGD5-AS1. *symbolizes $P < 0.05$, **symbolizes $P < 0.01$, and ***symbolizes $P < 0.001$

vein injection to evaluate the metastatic potential of OC cells in vivo. The results suggested that the knockdown of FGD5-AS1 reduced the lung metastasis of OC cells (Fig. 7g, Table 3).

Discussion

LncRNA is mainly transcribed by RNA polymerase II and lacks an open reading frame [26]. LncRNA's abnormal expression and its mutations can facilitate or repress tumorigenesis and cancer metastasis, and have potential significance in cancer diagnosis and treatment [27–29]. For example, compared with early OC (stage I/II), lncRNA ZFAS1 expression is higher in high-stage OC patients (stage III/IV); furthermore, the high expression of ZFAS1 is related with a shorter overall survival time and disease-free survival time of OC patients [30]. LncRNA DANCR promotes

the progression of OC by reducing UPF1 expression [31]. FGD5-AS1 has been reported to function as an oncogenic lncRNA in colorectal cancer, oral cancer, lung cancer and esophageal squamous cell carcinoma [32–35]. This study, for the first time, reported that FGD5-AS1 was highly expressed in OC tumor tissues and cell lines. Moreover, its high expression was correlated with T stage and lymph node metastasis of OC patients. Furthermore, in vitro and in vivo experiments demonstrated that FGD5-AS1 regulated the proliferation as well as metastasis of OC cells. The above results suggested that FGD5-AS1 was a new cancer-promoting factor in OC.

In recent years, more and more researches have shown that the up-regulation or down-regulation of miRNA expression can act on different targets or pathways and thus affect the occurrence, development, and metastasis of tumors [36]. miR-142-5p, one of the important members of the miRNA family, represses the proliferation of
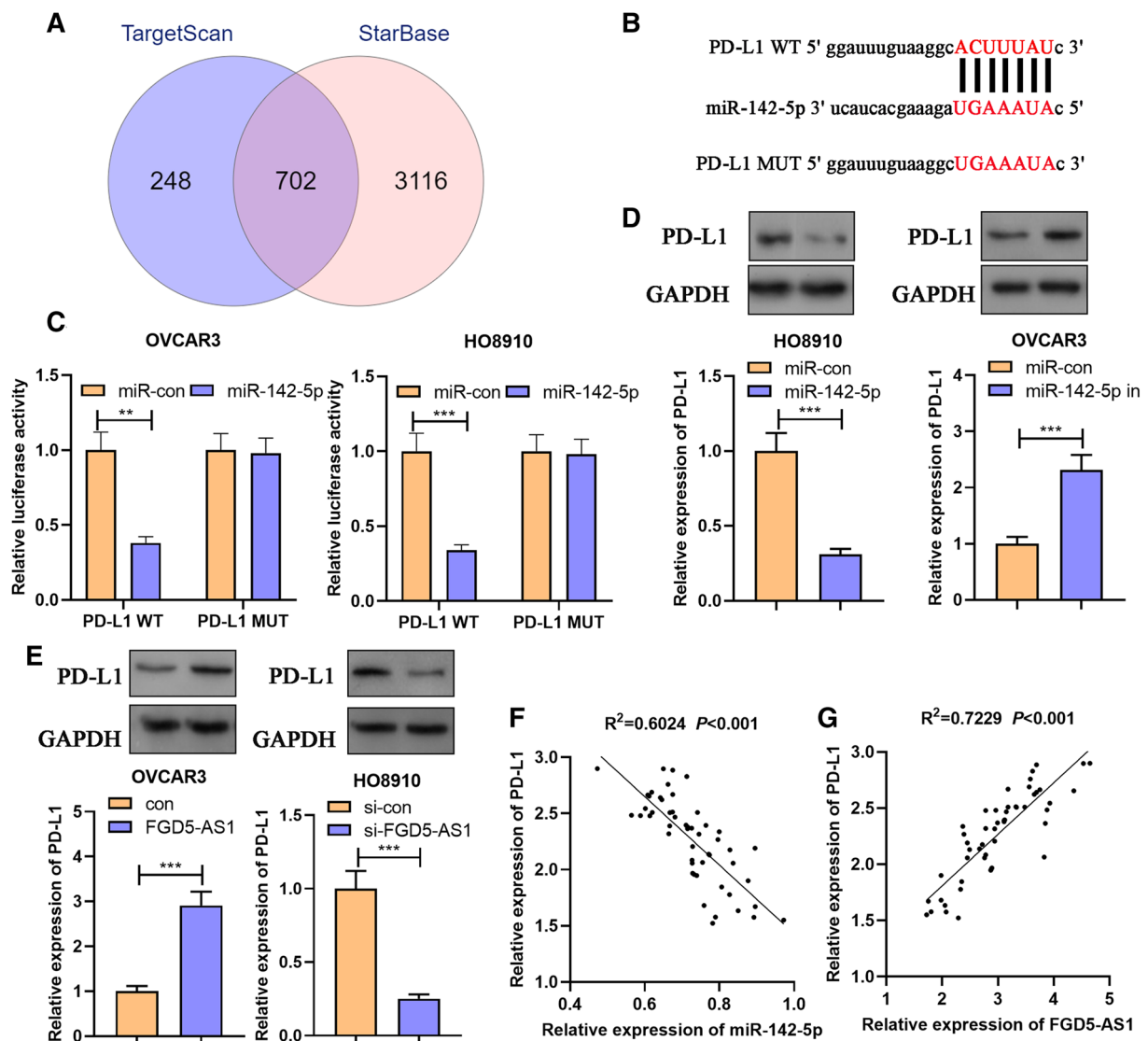
Fig. 6 PD-L1 is the direct or indirect target of miR-142-5p in OC. **a** Venn diagrams of putative miR-142-5p targets predicted by TargetScan and StarBase. **b** The binding site between miR-142-5p and PD-L1 was shown. **c** Dual luciferase report assay suggested that miR-142-5p could repressed the luciferase activity of wild type PD-L1 reporter, but had no significant impact on the luciferase activity of mutant type PD-L1 reporter. **d** and **e** Western blor and RT-PCR was employed to detect PD-L1 expression in OC cell lines after the selective up-regulation or down-regulation of FGD5-AS1 or miR-142-5p. **f** The expression level of miR-142-5p was negatively correlated with the expression level of PD-L1 in OC samples. **g** The expression level of PD-L1 was positively correlated with the expression level of FGD5-AS1 in OC samples. **symbolizes $P < 0.01$, and ***symbolizes $P < 0.001$

pancreatic cancer cells and facilitates apoptosis by negatively regulating the expression of RAP1A [37]. In OC, miR-142-5p targets a variety of anti-apoptotic genes, such as BIRC3, BCL2, BCL2L2, as well as MCL1, modulating the apoptosis and chemosensitivity to cisplatin of cancer cells [38, 39]. These studies illustrate that miR-142-5p exerts a tumor-suppressive impact on cancer progression. The present study reported that miR-142-5p overexpression markedly repressed the proliferation and metastasis of OC cells, which is consistent with the previous reports.

LncRNA, as competitive endogenous RNA (ceRNA), can modulate gene expression by competitively binding with miRNA as a molecular sponge and thus repressing its function. For example, lncRNA GICHG absorbs miRNA-1281 to facilitate the malignant progression of breast cancer [40]; lncRNA OIP5-AS1 promotes the proliferation of gastric cancer cells by targeting miR-641 [41]. This study found that FGD5-AS1 played a cancer-promoting role in OC, whereas miR-142-5p had an anti-cancer effect. It was supposed that ceRNA mechanism may also exist between FGD5-AS1 and miR-142-5p.
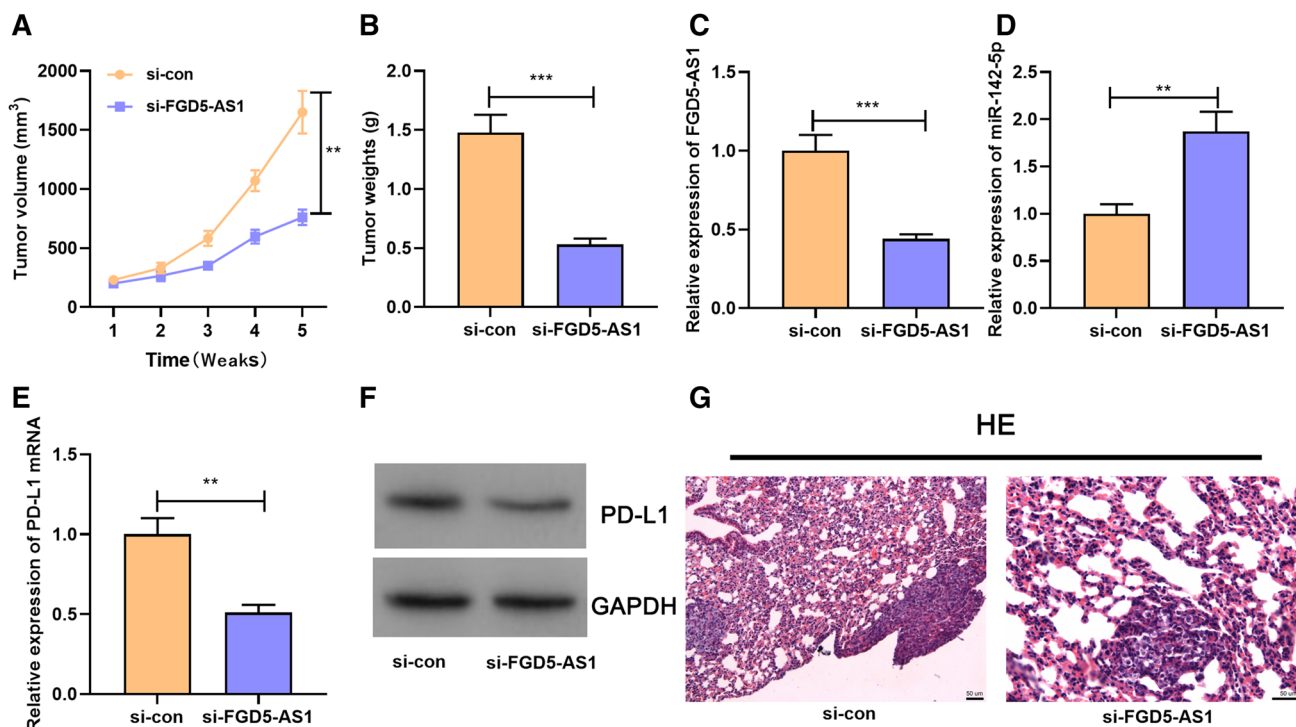
Fig. 7 Knockdown of FGD5-AS1 repressed tumor proliferation and metastasis in vivo. **a, b** Knocking down FGD5-AS1 repressed the growth of tumor weight and volume in vivo. **c–e** RT-PCR was employed to investigate the expressions of FGD5-AS1, miR-142-5p, and PD-L1 in tumor tissues of the mice. **f** Western blot was utilized to quantify PD-L1 expression in tumor tissues. **g** HE staining was utilized to detect lung metastasis of the mice. **symbolizes $P < 0.01$, and ***symbolizes $P < 0.001$

In the present work, the binding site was predicted between FGD5-AS1 and miR-142-5p through bioinformatics analysis. Luciferase reporter gene assay and RIP experiment confirmed that FGD5-AS1 could adsorb miR-142-5p. What's more, FGD5-AS1 overexpression impeded the expression of miR-142-5p; conversely, knocking down FGD5-AS1 increased the expression level of miR-142-5p. Furthermore, the promoting effects of FGD5-AS1 on OC malignant phenotypes could be partially attenuated by miR-142-5p. It was concluded that FGD5-AS1 was involved in the regulation of OC cell proliferation, migration, as well as invasion by functioning as a molecular sponge for miR-142-5p.

PD-L1, as an important immunosuppressive factor, becomes a predictive biomarker in cancer immunotherapy and plays crucial roles in the progression of different malignant tumors, including but not limited to melanoma, lung cancer, kidney cancer, bladder cancer, as well as OC [42, 43]. The bi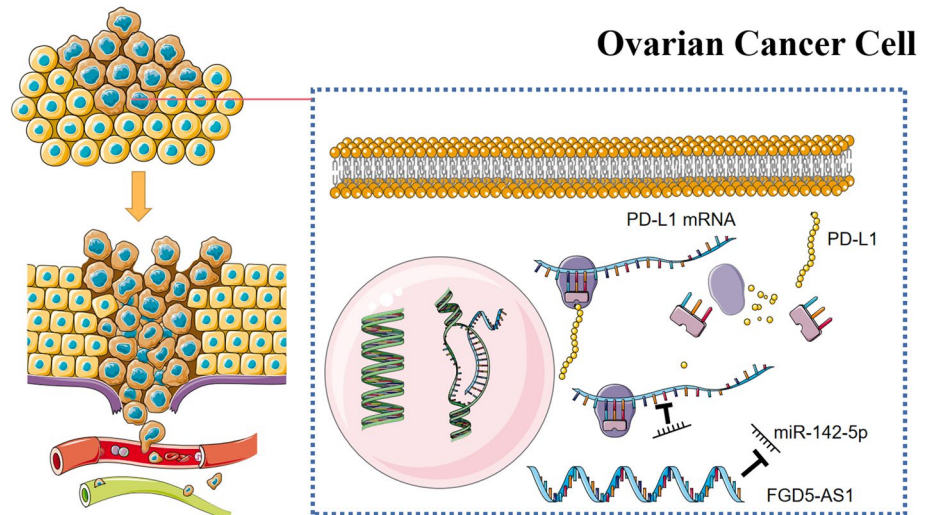nding between PD-L1 on the surface of tumor cells and PD-1 on T cells can repress T cell proliferation, reduce T cell activation, and make Th2 predominate in the tumor microenvironment, thus resulting in tumor immune escape [44]. Blocking PD1 or PD-L1 can restore T cell viability and its cytotoxicity, and induce a Th1 phenotype, thereby rejuvenating T cells to have stronger anti-tumor ability [44, 45]. In OC, PD-L1 stimulates IFN-γ and phosphorylates S6K, thereby facilitating OC cell proliferation and metastasis. In this process, IFN-γ stimulation can up-regulate the phosphorylation of AKT, while knocking out PD-L1 can repress IFN-γ-induced excessive activation of the AKT signaling pathway [46]. Additionally, previous studies have suggested that PD-L1 is negatively regulated by miR-142-5p [47, 48]. This study confirmed that FGD5-AS1 could adsorb miR-142-5p in OC. Therefore, it was concluded that the FGD5-AS1/miR-142-5p/PD-L1 axis was involved in facilitating OC progression.

To sum up, this study finds for the first time that FGD5-AS1 is highly expressed in OC tissues and cells. Moreover, its high expression is related to the adverse pathological indicators of OC patients. Mechanistically, it is confirmed that FGD5-AS1 facilitates cell proliferation, migration, as well as invasion through the miR-142-5p/PD-L1 axis (Fig. 8). FGD5-AS1 may be a new biomarker and therapy target for the diagnosis and treatment of OC.

Table 3 Degree of of lung metastasis in nude mice

	si-FGD5-AS1	si-NC	χ^2	p
Severe	8	3	5.0505	0.0246
Mild	2	7		

Fig. 8 Graphic abstract: FGD5-AS1 is significantly down-regulated in OC tissues and cell lines. In vitro and in vivo assays show that FGD5-AS1 accelerates OC cell proliferation, migration and invasion of OC cell. Mechanistically, it is revealed that FGD5-AS1 can increase PD-L1 expression via competitively binding with miR-142-5p in OC cells

Declarations

References

1. Zhao JL, Wang CL, Liu YL, Zhang GY (2019) Long noncoding RNA SNHG14 enhances migration and invasion of ovarian cancer by upregulating DGCR8. Eur Rev Med Pharmacol Sci 23(23):10226–10233

2. Zhu LY, Jia CH, Park E (2019) Research on characteristic manifestations of xiaochaihu decoction based on association rules mining. World J Tradit Chin Med 5(1):9–17

3. Wang J, Zheng M, Zhu L, Deng L, Li X Gao L, Wang C, Wang H, Liu J, Lin B (2019) Low BCL9 expression inhibited ovarian epithelial malignant tumor progression by decreasing proliferation, migration, and increasing apoptosis to cancer cells. Cancer Cell Int 19:330.

4. Soriano AA, de Cristofaro, Di Palma T, Dotolo S, Gokulnath P, Izzo A, Calì G, Facchiano A, Zannini M (2019) PAX8 expression in high-grade serous ovarian cancer positively regulates attachment to ECM via Integrin β3. Cancer Cell Int 19:303.

5. Gong M, Luo C, Meng H, Li S, Nie S, Jiang Y, Wan Y, Li H, Cheng W (2019) Upregulated LINC00565 accelerates ovarian cancer progression by targeting GAS6. Onco Targets Ther 12:10011–10022

6. Chen KX (2020) Academician kai-xian chen talks about the development of traditional chinese medicine and global medicine. World J Tradit Chin Med 6(1):1–11

7. Xun J, Wang C, Yao J, Gao B, Zhang L (2019) Long non-coding RNA HOTAIR modulates KLF12 to regulate gastric cancer progression via PI3K/ATK signaling pathway by sponging miR-618. Onco Targets Ther 12:10323–10334

8. Zhang Y, Zhang P, Chen L, Zhao L, Zhu J, Zhu T (2019) The Long Non-Coding RNA-14327.1 Promotes migration and invasion potential of endometrial carcinoma cells by stabilizing the potassium channel Kca3.1. Onco Targets Ther 12:10287–10297.

9. Li N, Yang G, Luo L, Ling L, Wang X, Shi L, Lan J, Jia X, Zhang Q, Long Z, Liu J, Hu W, He Z, Liu H, Liu W, Zheng G (2020) LncRNA THAP9-AS1 promotes pancreatic ductal adenocarcinoma growth and leads to a poor clinical outcome via sponging miR-484 and interacting with YAP. Clin Cancer Res 26(7):1736–1748

10. Wang J, Xing H, Nikzad AA, Liu B, Zhang Y, Li S, Zhang E, Jia Z (2020) LncRNA MNX1-AS1 exerts oncogenic functions in bladder cancer by regulating miR-218-5p/RAB1A axis. J Pharmacol Exp Ther 372(3):237–247

11. Wang D, Wu W, Huang W, Wang J, Luo L, Tang D (2019) LncRNA LUADT1 sponges miR-15a-3p to upregulate Twist1 in small cell lung cancer. BMC Pulm Med 19(1):246

12. Gokulnath P, de Cristofaro T, Manipur I, Di Palma T, Soriano AA, Guarracino MR, Zannini M (2019) Long non-coding RNA MAGI2-AS3 is a new player with a tumor suppressive role in high grade serous ovarian carcinoma. Cancers (Basel) 11(12)

13. Ma X, Liang AL, Liu YJ (2019) Research progress on the relationship between lung cancer drug-resistance and microRNAs. J Cancer 10(27):6865–6875

14. Yao G, Ying-Xia Z, Teng X, Jun-Sheng T, Xue-Mei Q (2020) Research progress on antidepressant therapeutic biomarkers of Xiaoyaosan. World J Tradit Chin Med 6(2):171–179

15. Liu X, Shao Y, Zhou J, Qian G, Ma Z (2019) Nuclear factor κb signaling and its related non-coding rnas in cancer therapy. Mol Ther Nucleic Acids 19:208–217

16. Xu H, Zhao G, Zhang Y, Jiang H, Wang W, Zhao D, Hong J, Yu H, Qi L (2019) Mesenchymal stem cell-derived exosomal micro-RNA-133b suppresses glioma progression via Wnt/β-catenin signaling pathway by targeting EZH2. Stem Cell Res Ther 10(1):381

17. Guo S, Fesler A, Huang W, Wang Y, Yang J, Wang X, Zheng Y, Hwang GR, Wang H, Ju J (2019) Functional significance and therapeutic potential of miR-15a Mimic in pancreatic ductal adenocarcinoma. Mol Ther Nucleic Acids 19:228–239

18. Yu W, Li D, Zhang Y, Li C, Zhang C, Wang L (2019) MiR-142–5p acts as a significant regulator through promoting proliferation, invasion, and migration in breast cancer modulated by targeting SORBS1. Technol Cancer Res Treat 18:1533033819892264.

19. Jia Y, Duan Y, Liu T, Wang X, Lv W, Wang M, Wang J, Liu L (2019) LncRNA TTN-AS1 promotes migration, invasion, and epithelial mesenchymal transition of lung adenocarcinoma via sponging miR-142-5p to regulate CDK5. Cell Death Dis 10(8):573

20. Wan H, Ma H, Zhu S, Wang F, Tian Y, Ma R, Yang Q Hu Z3, Zhu T, Wang W, Ma Z, Zhang M, Zhong Y, Sun H, Liang Y, Dai H (2018) Developing a bright NIR-II fluorophore with fast renal excretion and its application in molecular imaging of immune checkpoint PD-L1. Adv Funct Mater 28(50)

21. Hays E, Bonavida B (2019) YY1 regulates cancer cell immune resistance by modulating PD-L1 expression. Drug Resist Updat 43:10–28

22. Sun JR, Zhang X, Zhang Y (2019) MiR-214 prevents the progression of diffuse large B-cell lymphoma by targeting PD-L1. Cell Mol Biol Lett 24:68

23. Zhao R, Song Y, Wang Y, Huang Y, Li Z, Cui Y, Yi M, Xia L, Zhuang W, Wu X, Zhou Y (2019) PD-1/PD-L1 blockade rescue exhausted CD8+ T cells in gastrointestinal stromal tumours via the PI3K/Akt/mTOR signalling pathway. Cell Prolif 52(3):e12571

24. Cao R, Song W, Ye C, Liu X, Li L, Li Y, Yao H, Zhou X, Li L, Shao R (2019) Internal enhancement of DNA damage by a novel bispecific antibody-drug conjugate-like therapeutics via blockage of mTOR and PD-L1 signal pathways in pancreatic cancer. Cancer Med 8(2):643–655

25. Qu QX, Xie F, Huang Q, Zhang XG (2017) Membranous and cytoplasmic expression of PD-L1 in ovarian cancer cells. Cell Physiol Biochem 43(5):1893–1906

26. Li J, Li Z, Zheng W, Li X, Wang Z, Cui Y, Jiang X (2017) LncRNA-ATB: an indispensable cancer-related long noncoding RNA. Cell Prolif 50(6).

27. Huang HW, Xie H, Ma X, Zhao F, Gao Y (2017) Upregulation of LncRNA PANDAR predicts poor prognosis and promotes cell proliferation in cervical cancer. Eur Rev Med Pharmacol Sci 21(20):4529–4535

28. Du QQ, Tang M, Huang LL, Zhao R, Yan C, Li Y (2020) The anti-tumor activity and mechanism of MCL3 in G422 glioblastoma. World J Tradit Chin Med 6:353–361

29. Ni H, Niu LL, Tian SC, Jing LK, Zhang LT, Lin QQ, Cai YH, Liang HM, Du Q, Li H (2019) Long non-coding RNA LINC00152 is up-regulated in ovarian cancer tissues and regulates proliferation and cell cycle of SKOV3 cells. Eur Rev Med Pharmacol Sci 23(22):9803–9813

30. Han S, Li DZ, Xiao MF (2019) LncRNA ZFAS1 serves as a prognostic biomarker to predict the survival of patients with ovarian cancer. Exp Ther Med 18(6):4673–4681

31. Pei CL, Fei KL, Yuan XY, Gong XJ (2019) LncRNA DANCR aggravates the progression of ovarian cancer by downregulating UPF1. Eur Rev Med Pharmacol Sci 23(24):10657–10663

32. Li D, Jiang X, Zhang X, Cao G, Wang D, Chen Z (2019) Long noncoding RNA FGD5-AS1 promotes colorectal cancer cell proliferation, migration, and invasion through upregulating CDCA7 via sponging miR-302e. Vitro Cell Dev Biol Anim 55(8):577–585

33. Lin JG, Lyu J, Sun MH, Liao X, Xie YM (2020) Systematic review and meta-analysis of shenfu injection on treating acute exacerbation of chronic obstructive pulmonary disease. World J Tradit Chin Med 6:276–283

34. Fan Y, Li H, Yu Z, Dong W, Cui X, Ma J, Li S (2020) Long non-coding RNA FGD5-AS1 promotes non-small cell lung cancer cell proliferation through sponging hsa-miR-107 to up-regulate FGFRL1. Biosci Rep 40(1)

35. Sheng J, Wang L, Han Y, Chen W, Liu H (2018) Dual roles of protein as a template and a sulfur provider: a general approach to metal sulfides for efficient photothermal therapy of cancer. Small 14(1):1702529.

36. Deb B, Uddin A, Chakraborty S (2018) miRNAs and ovarian cancer: an overview. J Cell Physiol 233(5):3846–3854

37. Yao R, Xu L, Wei B, Qian Z, Wang J, Hui H, Sun Y (2019) miR-142-5p regulates pancreatic cancer cell proliferation and apoptosis by regulation of RAP1A. Pathol Res Pract 215(6):152416

38. Li X, Chen W, Jin Y, Xue R, Su J, Mu Z, Li J, Jiang S (2019) miR-142-5p enhances cisplatin-induced apoptosis in ovarian cancer cells by targeting multiple anti-apoptotic genes. Biochem Pharmacol 161:98–112

39. Wang PU, Wang J, Tan H, Weng S, Cheng L (2018) Acid-and reduction-sensitive micelles for improving the drug delivery efficacy for pancreatic cancer therapy. Biomater Sci 6(5):1262–1270.

40. Fan LY, Shi KY, Xu D, Ren LP, Yang P, Zhang L, Wang F, Shao GL (2019) LncRNA GIHCG regulates microRNA-1281 and promotes malignant progression of breast cancer. Eur Rev Med Pharmacol Sci 23(24):10842–10850

41. Wang LW, Li XB, Liu Z, Zhao LH, Wang Y, Yue L (2019) Long non-coding RNA OIP5-AS1 promotes proliferation of gastric cancer cells by targeting miR-641. Eur Rev Med Pharmacol Sci 23(24):10776–10784

42. Patel SP, Kurzrock R (2015) PD-L1 expression as a predictive biomarker in cancer immunotherapy. Mol Cancer Ther 14(4):847–856

43. Liu SY, Wu YL (2019) Biomarker for personalized immunotherapy. Transl Lung Cancer Res 8(Suppl 3):S308–S317

44. Drakes ML, Mehrotra S, Aldulescu M, Potkul RK, Liu Y, Grisoli A, Joyce C, O'Brien TE, Stack MS, Stiff PJ (2018) Stratification of ovarian tumor pathology by expression of programmed cell death-1 (PD-1) and PD-ligand- 1 (PD-L1) in ovarian cancer. J Ovarian Res 11(1):43

45. Tumeh PC, Harview CL, Yearley JH, Shintaku IP, Taylor EJ, Robert L, Chmielowski B, Spasic M, Henry G, Ciobanu V, West AN, Carmona M, Kivork C, Seja E, Cherry G, Gutierrez AJ, Grogan TR, Mateus C, Tomasic G, Glaspy JA, Emerson RO, Robins H, Pierce RH, Elashoff DA, Robert C, Ribas A (2014) PD-1 blockade induces responses by inhibiting adaptive immune resistance. Nature 515(7528):568–571

46. Gao H, Zhang J, Ren X. PD-L1 regulates tumorigenesis and autophagy of ovarian cancer by activating mTORC signaling. Biosci Rep 2019 39(12)

47. Wan J, Ling X, Peng B, Ding G (2018) miR-142-5p regulates CD4+ T cells in human non-small cell lung cancer through PD-L1 expression via the PTEN pathway. Oncol Rep 40(1):272–282

48. Jia L, Xi Q, Wang H, Zhang Z, Liu H, Cheng Y, Guo X, Zhang J, Zhang Q, Zhang L, Xue Z, Li Y, Da Y, Zhao P, Zhang R (2017) miR-142-5p regulates tumor cell PD-L1 expression and enhances anti-tumor immunity. Biochem Biophys Res Commun 488(2):425–431